# Chapter 9
# Bandgap Design of Metamaterial Structures by Varying Local Resonator Properties

**Hannes Wöhler and Sebastian Tatzko**

**Abstract** The concept of metamaterials can be used in structural dynamics to reduce vibrations. By attaching local resonators of given eigenfrequency to a host structure, a so-called bandgap is created which indicates significant vibration reduction in a broad frequency range. Although the resonators are basically represented by spring-mass systems the bandgap phenomenon goes beyond the well-known tuned mass damper behavior. This is due to the fact that the resonators are positioned at different locations of the host structure. It is well known that by increasing the mass of the resonators, the band gap width also increases. However, adding weight is not always a viable option when it comes to lightweight structures for example.

In this study we investigate new ways to increase the bandgap width without adding mass to the metamaterial structure. We consider a set of resonators for which we change individual stiffness values and investigate different arrangements of the eigenfrequency distribution of the resonators while keeping the total mass constant. The resonators influence the host structure dynamics and can be seen as a band-pass filter for mechanical waves which offers various possible applications in the field of vibration mitigation.

**Keywords** Metamaterial · Bandgap · Local resonators · Detuning · Mechanical filter

## Introduction

In the field of structural dynamics, the use of the bandgap effect of metamaterials to attenuate vibrations is a current topic in research and development. Metamaterials consisting of a periodic e.g. geometric pattern generally offer a so-called phononic bandgap [1], which is in principle located in the higher frequency range. The origin of this effect can be traced back to research on phononic crystals [2]. Another approach is to add local resonators in a periodic pattern to a host structure, where traditionally resonators tuned to identical frequencies are distributed across the structure. This also creates a bandgap, which in this case is based on the so-called resonator effect. The big advantage for structural dynamics is that the usual bandgap is in a much lower frequency range. It is determined by the arrangement and properties of the resonators [3–5].

Recent research has extended this approach by exploring variations in resonator tuning to achieve multiple [6] and wider bandgaps [7, 8]. One such concept is a series of differently tuned resonators to cover broader frequency ranges. This study builds on by proposing systematic detuning patterns of resonators attached to a segment of a host structure. The main goal is to increase the bandgap width by employing different configurations of resonator detuning.

To investigate the effectiveness of these configurations, we use a basic lumped-mass model that serves as a simplified framework for analyzing different metamaterial arrangements. The study examines several detuning patterns, including alternating and linearly in-/ decreasing triangular formations, each with three levels of detuning. In addition, we compare the calculated bandgap widths of these finite lumped-mass models with those obtained from the Bloch's theorem model, which uses a unit cell with complex boundary conditions to calculate a dispersion diagram [9, 10].

Hannes Wöhler · Sebastian Tatzko
Institute of Dynamics and Vibration Research, Leibniz University Hannover, An der Universität 1, 30823 Garbsen, Germany
e-mail: woehler@ids.uni-hannover.de; tatzko@ids.uni-hannover.de



Matthew Allen et al. (eds.), *Special Topics in Structural Dynamics & Experimental Techniques, Vol. 5*, Conference Proceedings of the Society for Experimental Mechanics Series, https://doi.org/10.13052/97887-438-0150-4_9

## Modeling of Metamaterial Structure

This work is based on a metamaterial model consisting of a lumped-mass system, which is described via mass matrix $\boldsymbol{M}$, damping matrix $\boldsymbol{C}$ and stiffness matrix $\boldsymbol{K}$. In this structure, the resonator effect is utilized to achieve a bandgap considering the displacement amplitudes from one end to the other. Figure 1 shows that seven resonators are coupled to the central part of the host structure which is an oscillator chain with 15 degrees of freedom (DOFs). Each host mass is coupled to the environment via a linear spring. The whole metamaterial structure is base excited via stiffness at the first DOF $x_{\mathrm{exc}}$.

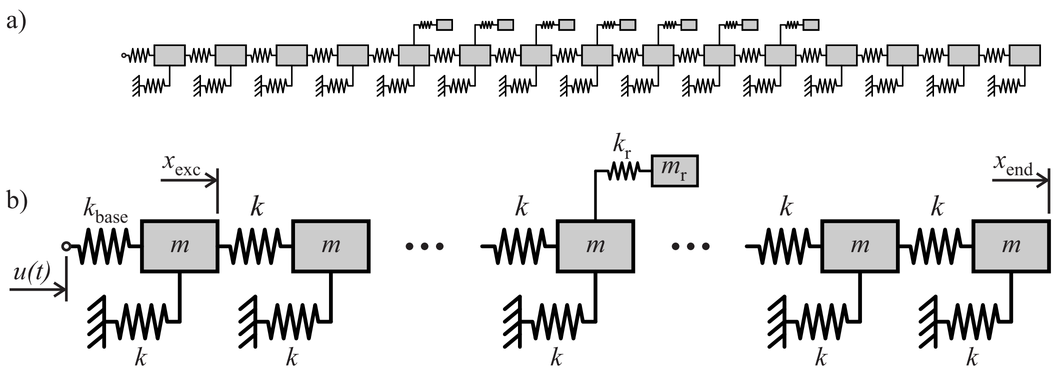


**Fig. 1** Lumped-mass model of the metamaterial structure with base excitation: a) full system with 15 host masses and seven resonators; b) detailed view of parts with labeling.

Table 1 shows the parameters of the lumped-mass model of the metamaterial structure in Figure 1. The resonator masses of the reference model are 10 % of the host masses $m_{\mathrm{r}} = 0.1 \cdot m$ for which a significant bandgap is already observed. For comparison, the resonator masses are doubled in another variant to 20 % of the host masses $m_{\mathrm{r}} = 0.2 \cdot m$ to show the effect of bandgap enlargement by simply adding mass. Figure 1 does not show any dashpot dampers, but they are modeled proportional to the stiffnesses $k$ and $k_{\mathrm{r}}$ using Rayleigh-damping in the form of $\boldsymbol{C} = \beta \boldsymbol{K}$.

**Table 1** Parameters of lumped-mass model and equally tuned resonators, cf. Figure 1.

| | $k_{\mathrm{base}}$ in $\frac{\mathrm{N}}{\mathrm{m}}$ | $m$ in kg | $c$ in $\frac{\mathrm{Ns}}{\mathrm{m}}$ | $k$ in $\frac{\mathrm{N}}{\mathrm{m}}$ | $m_{\mathrm{r}}$ in kg | $c_{\mathrm{r}}$ in $\frac{\mathrm{Ns}}{\mathrm{m}}$ | $\omega_{\mathrm{r}}$ in $\frac{\mathrm{rad}}{\mathrm{s}}$ | $k_{\mathrm{r}}$ in $\frac{\mathrm{N}}{\mathrm{m}}$ |
|---|---|---|---|---|---|---|---|---|
| equal (reference) | 1000 | 0.1 | $1.5 \cdot 10^{-7}$ | 8000 | 0.01 | $15 \cdot 10^{-7}$ | 440 | 1936 |
| equal 2-mass | 1000 | 0.1 | $1.5 \cdot 10^{-7}$ | 8000 | 0.02 | $15 \cdot 10^{-7}$ | 440 | 3872 |

The focus is on investigating the influence of different resonator detuning patterns with respect to the bandgap width at DOF $x_{\mathrm{end}}$. Figure 2 shows the different detuning patterns as bar plots. The metamaterial structure with seven resonators of equal mass each tuned via stiffnesses $k_{\mathrm{r}}$ to the natural frequency of $\omega_{\mathrm{r},1-7} = 440\ \frac{\mathrm{rad}}{\mathrm{s}}$ serves as a reference, see Figure 2 a). Two different detuning patterns with five detuning levels each are investigated for the seven resonators. On the one hand, an alternating ABABABA-pattern, in which the resonators are detuned by $\pm 5$ % ($\pm 10$ %, $\pm 15$ %, $\pm 20$ %, $\pm 25$ %) in relation to the base frequency of $440\ \frac{\mathrm{rad}}{\mathrm{s}}$. These are referred to as AB-5, AB-10, AB-15, AB-20 and AB-25, see Figure 2 b)-f).

On the other hand, a triangular Tri-tuning in the form of ABCDCBA is investigated. Here, resonators #1 and #7 are detuned by $-5$ % ($-10$ %, $-15$ %, $-20$ %, $-25$ %) and resonator #4 by $+5$ % ($+10$ %, $+15$ %, $+20$ %, $+25$ %). The resonators in between are detuned according to linear interpolation. The latter variants are referred to as Tri-5, Tri-10, Tri-15, Tri-20 and Tri-25, see Figure 2 h) - l). Note that the resonator masses for all configurations of patterns AB-tuning and Tri-tuning are equal to the resonator mass of the reference structure. This way the resonator masses stay unchanged and the bandgap width is only affected by detuning and not by mass effect. The eigenfrequency is thus only set via the resonator stiffnesses $k_{\mathrm{r}}$.

## Analysis of Bandgap Properties

The analysis of the band gap properties with regard to the band gap width is carried out in two ways, which are explained in the following section. First, the bandgap width will be determined by modeling the metamaterial structure as a unit cell

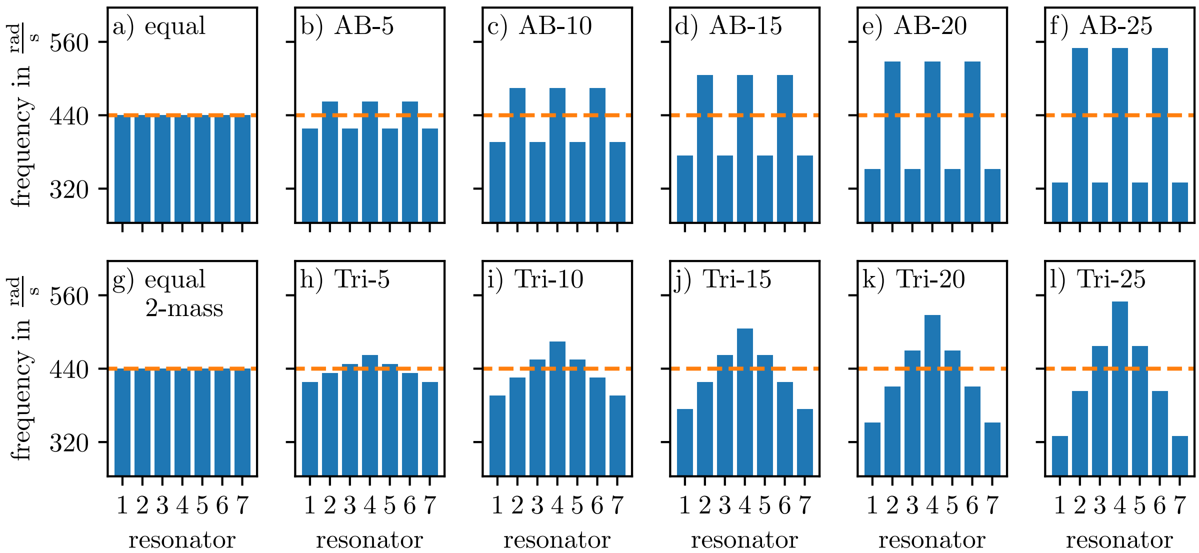


**Fig. 2** Configurations of metamaterial structure with seven resonators with base angular frequency of 440 $\frac{\mathrm{rad}}{\mathrm{s}}$: a) equally tuned; b) - f) with alternating AB-pattern at 5 %, 10 %, 15 %, 20 % and 25 % detuning level; g) equally tuned with doubled resonator mass; h) - l) with triangular pattern at 5 %, 10 %, 15 %, 20 % and 25 % detuning level.

model using Bloch's theorem. In a second approach, a method can be used in which the displacement transmissibility is calculated in order to obtain the bandgap width.

### *Bandgap width approximation via Bloch's theorem*

The bandgap properties of periodic metamaterial structures are often determined using Bloch's theorem [9]. For this purpose, complex boundary conditions with continuous phase shifts $\mu$ between 0 and $\pi$ (rad) are applied to the so-called unit cell. This is equivalent to an infinite repetition of this unit cell. For each phase shift $\mu$, an eigenvalue problem of the Bloch matrices $\boldsymbol{M}_{\mathrm{Bloch}}(\mu)$ and $\boldsymbol{K}_{\mathrm{Bloch}}(\mu)$ must be solved [10]. This method is comparatively fast and computationally efficient, as it reduces the problem dimension to its unit cell representation. This type of bandgap calculation has however the following disadvantages: edge reflections of finite structures are not taken into account, detuning of the resonators cannot be mapped and resonators that are not evenly distributed over the host structure cannot be represented either. Nevertheless, the Bloch's theorem based calculation of the bandgap provides useful results with regard to the general design of a metamaterial structure. Figure 3 shows in a) the unit cell of the reference metamaterial structure with the parameters of equally tuned resonators (equal) and in b) the corresponding dispersion diagram. The blue line belongs to the square root of the first eigenvalues $\omega_1(\mu)$, while the orange line belongs to the square root of the second eigenvalues $\omega_2(\mu)$. The angular eigenfrequency of the resonator $\omega_{\mathrm{r}}$ is shown as a dashed black line and the gray band refers to the bandgap, where no eigenvalues exist, which causes significant reductions in vibrations amplitudes transferred to the finite metamaterial structure with resonators. The calculated width of the bandgap via Bloch's theorem is 51.0 $\frac{\mathrm{rad}}{\mathrm{s}}$ and serves as a first reference for a corresponding finite metamaterial oscillator.

### *Bandgap width calculation via transmissibility*

Another way to quantify the bandgap width is to use the transmissibility method presented in this paper. Figure 4 a) shows the displacement amplitudes of the DOFs $x_{\mathrm{exc}}$ and $x_{\mathrm{end}}$ of the base excited host structure without resonators in comparison to the displacements of the reference metamaterial structure in b). It is clearly seen that there is an anti-resonance at 440 $\frac{\mathrm{rad}}{\mathrm{s}}$, which is the natural angular frequency of the resonators. Besides, the displacement amplitudes of $x_{\mathrm{end}}$ are significantly lower than those of $x_{\mathrm{exc}}$ in a broad frequency range around the resonator's natural frequency. The shape is significantly wider compared to a typical anti resonance. Figure 4 c) shows the transmissibility in dB

$$T(\Omega) = 10 \cdot \log\left(\frac{|\hat{x}_{\mathrm{end}}(\Omega)|}{|\hat{x}_{\mathrm{exc}}(\Omega)|}\right) \quad , \tag{1}$$

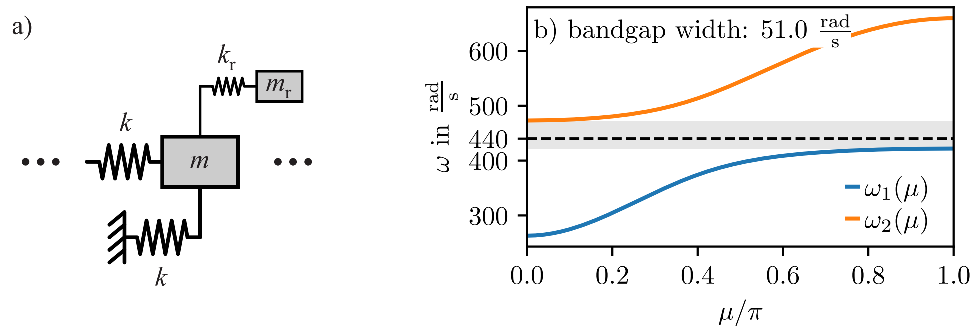


**Fig. 3** Analyzing of bandgap width by unit cell approach using Bloch's theorem: a) lumped-mass model of unit cell; b) resulting dispersion diagram with dispersion curves $\omega_1(\mu)$ and $\omega_2(\mu)$ and bandgap (gray box).

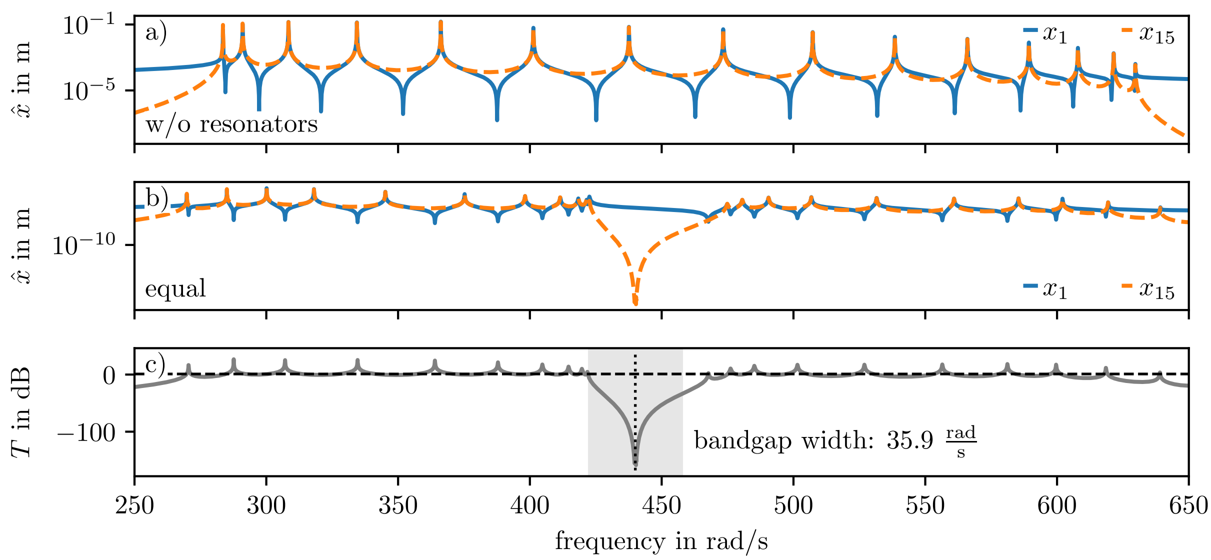


**Fig. 4** Calculation of bandgap width via transmissibility: a) displacement amplitudes $x_{\mathrm{exc}}$ and $x_{\mathrm{end}}$ of host structure without resonators; b) displacement amplitudes $x_{\mathrm{exc}}$ and $x_{\mathrm{end}}$ of metamaterial structure (equal); c) corresponding transmissibility $T$ for the configuration equal: gray box marks identified bandgap, vertical dotted line marks center of bandgap at resonator's base frequency of 440 $\frac{\mathrm{rad}}{\mathrm{s}}$.

which provides a robust basis for calculating the bandgap width of a finite metamaterial structure using e.g. displacement amplitudes. The bandgap is defined by values of $T(\Omega) < 0$ dB near the resonator's base natural frequency. Another criterion is that the identified bandgap width is centered at the resonator's natural frequency to avoid biased result in bandgap evaluation. Consider a desired bandgap at frequency $f_0$ for which the goal is reduced to just increase bandgap width. One may end up with a large bandgap onesided to either high or low frequency values. For meaningful results, we therefore introduce this symmetry constraint. The bandgap width calculated via transmissibility is 35.9 $\frac{\mathrm{rad}}{\mathrm{s}}$. In comparison, by applying the symmetry contraint to the identified bandgap information using Bloch's theorem in Figure 3 b), the adjusted bandgap width is 36.0 $\frac{\mathrm{rad}}{\mathrm{s}}$ instead of 51.0 $\frac{\mathrm{rad}}{\mathrm{s}}$ without symmetry constraint.

## Results of Bandgap Design

Twelve metamaterial variants are analyzed with regard to their bandgap widths. The bandgap width is determined using the transmissibility method described above, as Bloch's theorem is not applicable due to the more complex detuning patterns of the resonators. The identified bandgap widths of the investigated configurations are shown in Figure 5. The relative bandgap

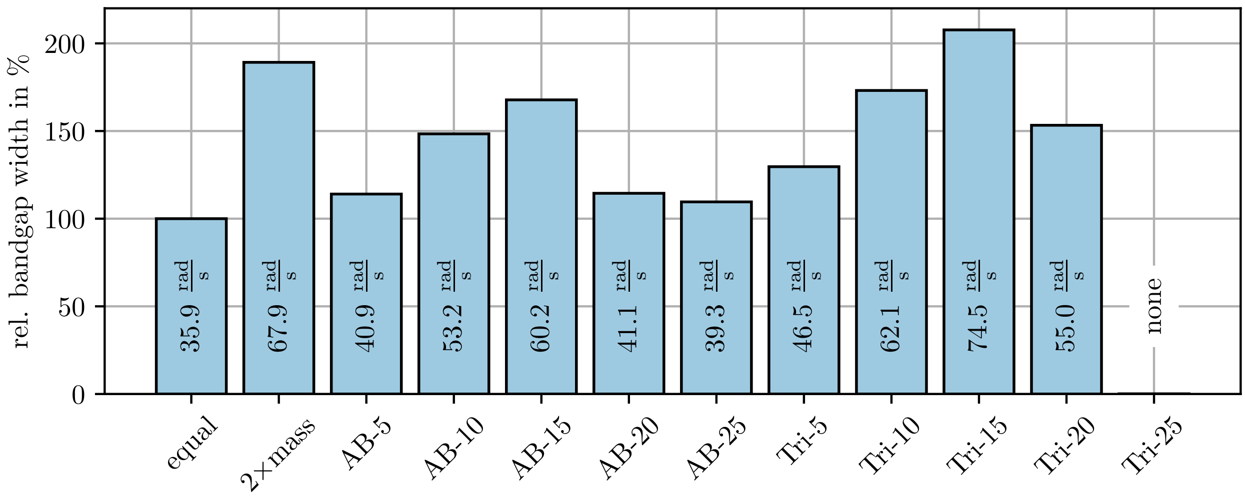


**Fig. 5** Bandgap widths at different metamaterial configurations calculated via displacement relation method.

width is also shown, where 100 % corresponds to the reference configuration (equal) with 35.9 $\frac{\mathrm{rad}}{\mathrm{s}}$. By using resonators that are twice as heavy but equally tuned, the bandgap can be widened, achieving a relative width of 189.2 %.

As increasing the mass of the resonators may not always be a feasible option, the bandgap width can also be influenced by systematically detuning the resonators holding the mass constant. In this study, two detuning patterns - alternating AB-tuning and triangular-tuning - each with five levels of detuning are analyzed for their potential to widen the bandgap, see Figure 2.

For the AB configurations AB-5, AB-10 and AB-15, an increase in the bandgap width compared to the reference is observed as the detuning level increases, see Figure 5. However, if the detuning level is increased further to 20 % or 25 %, the bandgap width is reduced again due to anti resonance phenomena as shown in the following.

Figure 6 shows in a) the displacement amplitudes at $x_{\mathrm{exc}}$ and $x_{\mathrm{end}}$ and in b) the corresponding transmissibility $T$. These plots visualize the drop in bandgap width of the configuration with $\pm$ 20 % detuned resonators. Looking at $x_{\mathrm{end}}$ in a), vibration response levels are reduced in a wide frequency range. The transmissibility however reveals due to an anti resonance of $x_{\mathrm{exc}}$ a local peak at $\approx$ 460 $\frac{\mathrm{rad}}{\mathrm{s}}$ at a certain degree of detuning. As we are interested in a bandgap around 440 $\frac{\mathrm{rad}}{\mathrm{s}}$, this phenomenon creates a new limit and corresponding sudden drop in effective bandgap width. The design of

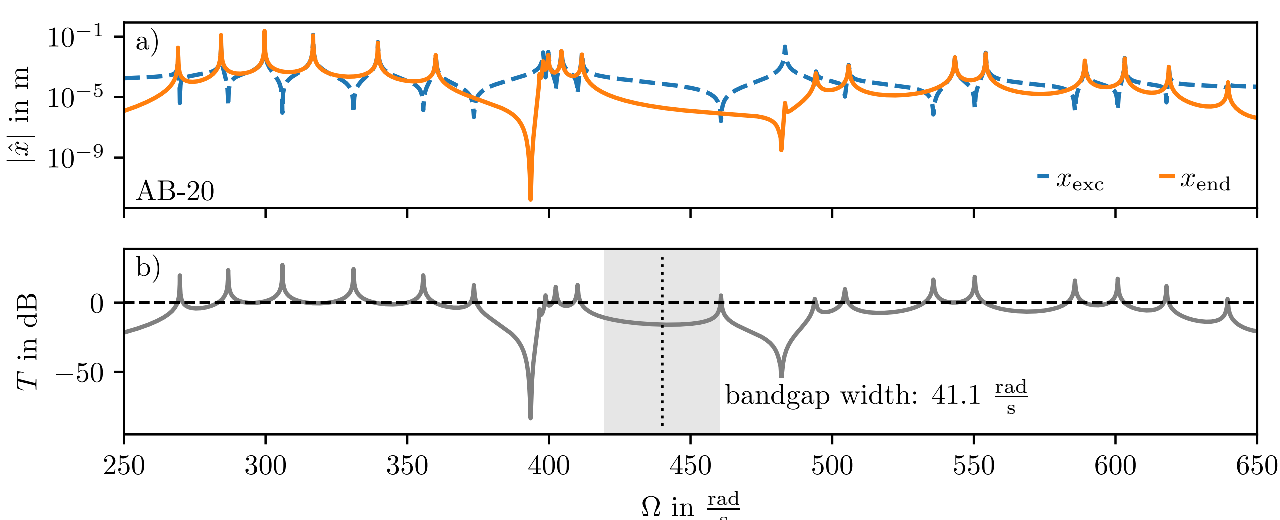


**Fig. 6** Configuration AB-20: a) displacement amplitudes $x_{\mathrm{exc}}$ and $x_{\mathrm{end}}$; b) corresponding transmissibility $T$.

metamaterial structures with respect to multiple bandgaps using different types of resonators is described in [6] and beyond the scope of the current work.

The variants with triangular detuning exhibit an increase in bandgap width up to $15\ \%$ detuning level. Notably, the Tri-15 configuration results in the widest relative bandgap of 207.7 %, surpassing even the configuration with doubled resonator mass, see Figure 7. This is particularly remarkable considering the aforementioned limitations of increasing resonator mass. It should be emphasized that no bandgap could be identified in the Tri-25 configuration, as the transmissibility is greater than 0 dB at the resonator's base frequency of $440\ \frac{\mathrm{rad}}{\mathrm{s}}$ and the bandgap criterion is therefore not fulfilled.

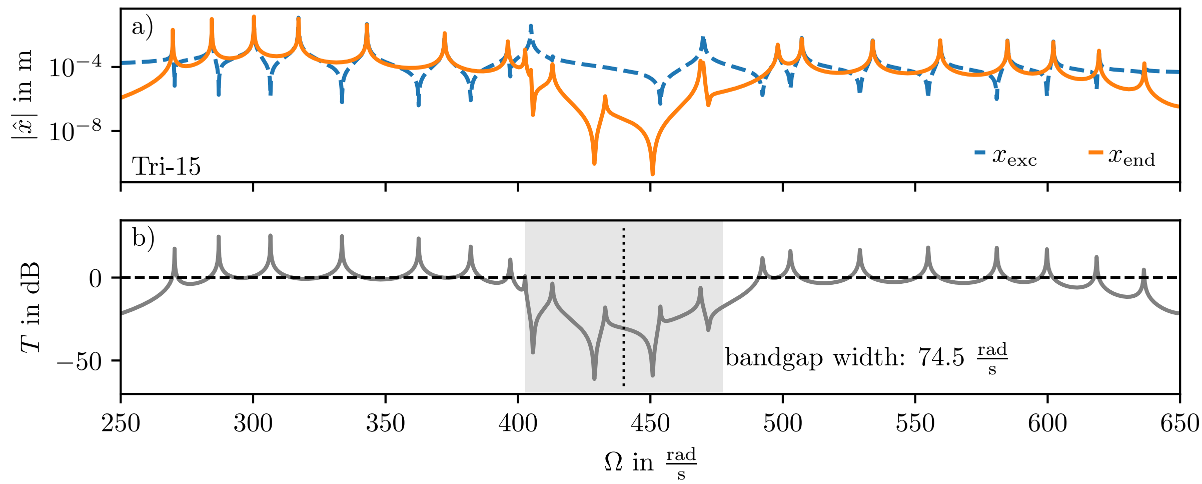


**Fig. 7** Configuration Tri-15: a) displacement amplitudes $x_{\mathrm{exc}}$ and $x_{\mathrm{end}}$; b) corresponding transmissibility $T$.

## Conclusion

In conclusion, the study investigates the effects of different detuning patterns on the bandgap width of a metamaterial structure with seven resonators, compared to the reference case of uniformly tuned resonators. It is well known that increasing the mass of the resonators results in an increased bandgap width. However, the focus of this work is to explore how detuning patterns, specifically an alternating detuning AB-pattern and a triangular detuning Tri-pattern, impact the bandgap width. The results demonstrate that a particular detuning pattern can achieve a wider bandgap than what could be attained merely by using heavier resonators. This insight is significant for the design and optimization of metamaterial structures, potentially leading to improved performance in various applications by strategically adjusting the detuning of resonators rather than solely relying on changes in mass.

**Acknowledgments** This work was funded by the Deutsche Forschungsgemeinschaft (DFG, German Research Foundation) – 462650249.

## References

1. Brillouin, L. *Wave Propagation in Periodic Structures*. Dover Publications Inc. (1953)
2. Yablonovitch, E. and Gmitter, T.J. "Photonic band structure: The face-centered-cubic case". *Physical Review Letters*, 63(18):1950–1953 (1989)
3. Liu, Z., Zhang, X., Mao, Y., Zhu, Y.Y., Yang, Z., Chan, C.T., and Sheng, P. "Locally resonant sonic materials". *Science*, 289(5485) (2000)
4. Wang, G., Wen, J., and Wen, X. "Quasi-one-dimensional phononic crystals studied using the improved lumped-mass method: Application to locally resonant beams with flexural wave band gap". *Physical Review B*, 71(10) (2005)
5. Lazarov, B. and Jensen, J. "Low-frequency band gaps in chains with attached non-linear oscillators". *International Journal of Non-Linear Mechanics*, 42(10) (2007)
6. Claeys, C., Rocha de Melo Filho, N.G., Van Belle, L., Deckers, E., and Desmet, W. "Design and validation of metamaterials for multiple structural stop bands in waveguides". *Extreme Mech. Lett.*, 12:7–22 (2017)
7. Celli, P., Yousefzadeh, B., Daraio, C., and Gonella, S. "Bandgap widening by disorder in rainbow metamaterials". *Applied Physics Letters*, 114(9) (2019)

8. Meng, H., Chronopoulos, D., Fabro, A.T., Elmadih, W., and Maskery, I. "Rainbow metamaterials for broadband multi-frequency vibration attenuation: Numerical analysis and experimental validation". *Journal of Sound and Vibration*, 465 (2020)
9. Bloch, F. "Über die Quantenmechanik der Elektronen in Kristallgittern". *Zeitschrift für Physik*, 52(7–8):555–600 (1929)
10. Frazier, M.J. and Hussein, M.I. "Generalized Bloch's theorem for viscous metamaterials: Dispersion and effective properties based on frequencies and wavenumbers that are simultaneously complex". *Comptes Rendus. Physique*, 17(5):565–577 (2016)